Plasma Chem Plasma Process (2013) 33:881–894
DOI 10.1007/s11090-013-9467-3

ORIGINAL PAPER

Plasma Treatment of Glass Surfaces Using Diffuse Coplanar Surface Barrier Discharge in Ambient Air

Tomáš Homola · Jindřich Matoušek · Martin Kormunda · Linda Y. L. Wu · Mirko Černák

Received: 31 January 2013 / Accepted: 22 June 2013 / Published online: 11 July 2013

Abstract We report a study on the treatment of flat glass surfaces by ambient air atmospheric pressure plasma, generated by a dielectric barrier discharge of coplanar arrangement of the electrode system—the diffuse coplanar surface barrier discharge (DCSBD). The plasma treatment of glass was performed in both static and dynamic modes. With respect to wettability of the glass surface, treatment in static mode resulted in non-uniform surface properties, whereas dynamic mode provided a fully uniform treatment. A water contact angle measurement was used to determine the efficiency of plasma treatments in dynamic mode and also to investigate a hydrophobic recovery of plasma treated glass surfaces. The X-ray photoelectron spectroscopy measurements showed a decrease of overall carbon concentrations after plasma treatment. A deconvolution of C1s peak, showed that a short plasma treatment led to decrease of C–C bonds concentration and increases of C–O and O–C=O bond concentrations. An enhancing influence of the glass surface itself on DCSBD diffuse plasma was observed and explained by different discharge onsets and changes in the electric field distribution.

Keywords Atmospheric pressure air plasma · DCSBD · Diffuse plasma · Glass surface · XPS

T. Homola (✉) · M. Černák
R&D Centre for Low-Cost Plasma and Nanotechnology Surface Modification, Masaryk University, Kotlářská 267/2, 61137 Brno, Czech Republic
e-mail: tomas.homola@mail.muni.cz

T. Homola · L. Y. L. Wu
Surface Technology Group, Singapore Institute of Manufacturing Technology, 71 Nanyang Drive, Singapore 638075, Singapore

J. Matoušek · M. Kormunda
Department of Physics, Faculty of Science, J.E. Purkinje University, České mládeže 8, 400 96 Ústí nad Labem, Czech Republic

M. Černák
Department of Experimental Physics, Faculty of Mathematics, Physics and Informatics, Comenius University, Mlynská dolina, 842 48 Bratislava, Slovakia

Introduction

Unique optical and physical properties designate glass for a use in numerous applications in several sectors of industry, including architecture, automotive, electronics, lighting, optics, the solar cells industry and many others [1–3]. In literature, many chemical methods for cleaning (and activation) of glass surfaces can be found [4–6]. Recently, these chemical methods are substituted by novel cold plasma methods, because plasma technologies are faster, cleaner and environmentally more attractive, compared to traditional chemical methods [7]. The plasma contains active particles (electrons, ions, excited and metastable particles, radicals and photons) in non-equilibrium states; thus they interact with glass surfaces and modify their chemical character.

Most of the scientific work on this method has been done with low pressure plasma. Plasma generators, operating at high pressures, including atmospheric pressure, allow faster, cheaper and more efficient treatment. A general problem with high pressure plasma (in comparison to low pressure plasma) consists in occurrence sparks and arcs that may cause point defects in surfaces during treatment. To prevent this, helium can be introduced into the discharge for stabilization [8], but its high cost is a limiting factor for practical use.

A different approach to non-thermal plasma generation at atmospheric pressure exists, using dielectric barrier discharges (DBD's) [9, 10]. An applied voltage of a few kV range at frequencies between 5 and 500 kHz is sufficient to create an active discharge region [11]. DBD's are often generated in a filamentary regime, which leads to considerable non-homogeneity in the treated surface areas. Ref. [12] shows results referring to the cleaning of glass surfaces by DBD plasma. It was found that a small amount (0.06 %) of O_2 in N_2 carrier gas plays an important role in the efficiency of carbon contaminant cleaning. Consequently, it was concluded that the cleaning of glass surfaces is driven mainly by the high oxidizing power of $O(^3P)$ radicals, whereas the influence of N-based species, especially N_2 ($A^3\sum u^+$) metastables, is negligible. However, since the stabilization of plasma was achieved by a high gas flow rate (up to 40 slm), the long-term consumption of N_2 gas can significantly increase the cost of the process.

A coplanar DBD plasma source, the diffuse coplanar surface barrier discharge (DCSBD) was used in this work to modify glass surfaces. The DCSBD generates a thin layer of non-equilibrium and diffuse plasma, with a high power density (up to order of 100 W/cm^3) in practically any type of working gas [13]. The coplanar arrangement of DBD for surface processing is very rare in the literature and even when it is used, the plasma is non-uniform and the maximum of power reached is only a few watts [14].

The primary difference between DCSBD and other plasma sources, tested for glass cleaning, consists in the fact that plasma is not generated within the inter-electrode volume but in a thin, flat layer above the system of electrodes on a dielectric surface which makes it ideal for the treatment of especially flat surfaces.

The DBD configurations, where plasma is generated in an inter-electrode volume, are limited by the required width between electrodes and the thickness of treated material, often used as a dielectric barrier, must be less than approximately 2 mm. Compared to a surface DBD setup that also generates a surface plasma [15], the advantage of DCSBD is that surface micro-discharges are not in a contact with the metallic electrodes and consequently, the electrode system has a practically unlimited lifetime.

When glass surfaces are exposed to plasma, two main processes are initiated. The first is a plasma cleaning of the organic contaminants, adsorbed on the glass surface, from the environment [16–18]. This process of contaminant removal is very important, e.g. for the manufacturing process of LCD's, where organic contamination encourages the formation

of electrostatic faults, such as the dielectric breakdown of deposited films onto glass [19]. It is also understood that surface contaminants may produce spots of non-homogeneity in coatings, resulting in imperfect adhesion between coatings and substrates [20]. The second process is the generation of hydrophilic oxygen-based polar groups, which can also govern the hydrophilic properties [21–23].

In this work, we mainly studied the treatment of glass surfaces by the ambient air DCSBD plasma, in order to remove carbon contaminants and increase wettability. Two different treatment modes are shown, with respect to homogeneity of the treatment and wettability changes. A study of influences of glass on DCSBD plasma is also presented here. X-ray photoelectron spectroscopy (XPS) was used to determine total amounts of carbon contamination on the glass surfaces, before and after plasma treatment.

Experimental

Materials

Flat soda-lime glass samples (Marienfeld GmbH, Germany), of 26 mm × 76 mm × 1 mm dimension, were treated by DCSBD plasma. Before plasma treatment, the samples were pre-cleaned by paper tissue, impregnated with 2-propanol (C_3H_8O) to ensure that each sample exhibited equal surface properties.

For better visualisation of the hydrophilic effect on glass treated by plasma, a 60 nm film of amorphous SiO_2, prepared from TEOS sol–gel dried at 50 °C, was deposited on the glass panes (10 cm × 10 cm × 2 mm).

Diffuse Coplanar Surface Barrier Discharge

The DCSBD system [24] (Roplass, Czech Rep.) is made from multiple parallel stripline molybdenum electrodes, embedded in 96 % alumina. The axonometric views of the DCSBD electrode system and its electrode profile are shown in Figs. 1 and 2, respectively. The actual number of electrodes in Figs. 1 and 2 was reduced to make this sketch clear. The dimensions of the alumina ceramic of the DCSBD system are $a = 93$ mm in width and $b = 230$ mm in height and the total plasma area is approximately 80 mm × 200 mm. The 16 pairs of molybdenum comb-shape electrodes (width and inter-electrode distance $c = 1.5$ mm and $d = 1$ mm, respectively), were printed by green-tape technique on a 0.5 mm thick ceramic plate.

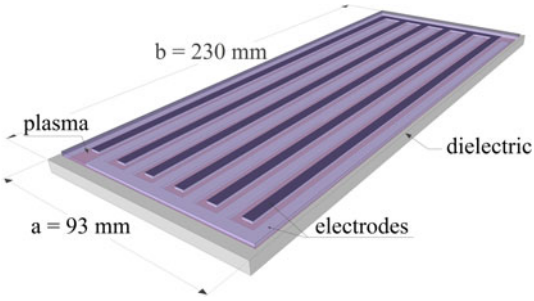

Fig. 1 Axonometric view of DCSBD electrode system

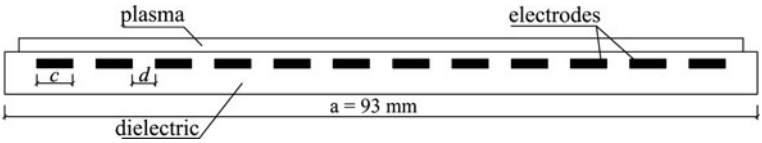

Fig. 2 Profile view of DCSBD electrode system

A high voltage AC power source, with peak to peak voltage up to 20 kV, at frequencies from 14 up to 18 kHz, was used to power the electrodes [13]. The maximum delivered power in the DCSBD plasma was reached at the resonance frequency of an electrode system, which is determined by its geometrical properties and capacitance. The resonance frequency was found by simultaneous increases in voltage and frequency sweeps. In this study, the DCSBD plasma was generated in an ambient air atmosphere with a delivered power 400 W, if not indicated otherwise.

The DCSBD plasma consists of numerous H-shaped luminous micro-discharges [25] that can be either static or travelling on a dielectric surface along embedded strip electrodes, their density varying from a single to many micro-discharge events produced per AC half-cycle [13]. The DCSBD micro-discharges are generated differently than those in volume DBD. Whereas standard volume DBD generates filamentary micro-discharges orientated perpendicularly to treated surface, the DSCBD produces micro-discharges parallel to the treated surface [26].

Glass–Plasma Influence

To study the influence of glass on DCSBD plasma with respect to glass–ceramic distance z, a glass pane (length 7 cm, thickness 1 mm) was placed on the ceramic surface of the DCSBD electrode system. The glass pane was lifted on its right side to $z = 0.75$ mm, whereas the left side remained in contact with the ceramic at $z = 0$ mm (see Fig. 3a). The photograph of influence between the glass and the DCSBD plasma was taken by a DSLR Canon EOS 500D, with Canon EFS 60 mm macro lens and UV filter. An ISO speed, an exposure time and an aperture were set to 200, 1/20 s and f/2.8, respectively. The point of view was located vertically above the ceramic surface. The photograph was optically modified by changes in the gamma correction from +1 to +1.5. Optimal contrast was reached without a background light in a laboratory. To prevent blurring, a tripod and external trigger were used.

To demonstrate the different behaviour of DBD plasma with respect to inter-electrode distance d, a planar volume-DBD arrangement was used. The bottom electrode (area approximately 20 cm × 10 cm) was made of an alumina and silver layer of thickness 0.5 mm and 40 μm, respectively. The counter electrode was made of glass and a transparent Indium-tin oxide (ITO) layer of thickness 2 mm and 120 nm, respectively. The counter electrode facing, with its ITO layer, was placed on the bottom electrode and lifted to $d = 0.75$ mm on the right side, whereas the left side remained in contact with the alumina ceramic at $d = 0$ mm (see Fig. 3b). The volume-DBD was driven by the same power source as the DCSBD, but the total power was only 150 W, instead of 400 W, in the DCSBD plasma. The photograph of the volume-DBD plasma was taken by the same camera as mentioned above. An ISO speed, exposure time and an aperture were set to 800, 1/60 s and f/2.8, respectively. No optical modifications were made to this photograph.

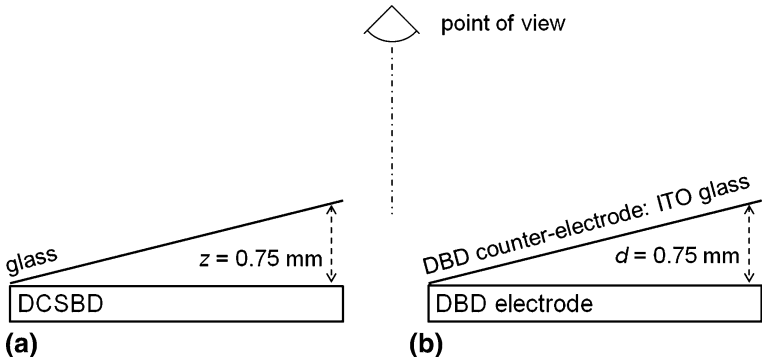

Fig. 3 Experimental setup of (**a**) glass-plasma influence visualisation with respect to glass–ceramic distance z and (**b**) DBD behaviour visualisation with respect to inter-electrode distance d

Plasma Treatment Methods

Two separate approaches were used in the treatment of glass samples. A static treatment mode was used to investigate the influence of the DCSBD plasma on the wettability of glass samples, with respect to the glass–ceramic distance z. The glass pane was placed on the DCSBD ceramic and lifted to $z = 0.8$ mm on the one side, whereas the other side remained in contact with the ceramic at $z = 0$ mm. The glass pane samples were treated by plasma for 5 s and wettability changes, with respect to the glass–ceramic distance z, were examined by water contact angle measurements along the surface.

The other glass samples used in this study were treated at dynamic mode, where the sample moved through the plasma layer above the dielectric surface at $z = 0.3$ mm, as described in [27]. To verify the homogeneity of plasma treatment in static and dynamic modes, the glass panes coated with SiO_2 were treated for 5 and 1 s in plasma, respectively, then immersed into distilled water for 5 s and subsequently removed. The homogeneity of the plasma treatment in static and dynamic modes was examined visually by changes in distribution of the water layer.

The durability of plasma treatment was investigated for glass samples treated for 6 s in the plasma at dynamic mode. After the treatment, samples were stored in an ambient air atmosphere of about 50 % relative humidity and a temperature about 20 °C. The water contact angles on glass samples were measured daily, for 5 days.

The glass samples investigated by XPS were also treated at dynamic mode for various times from 1 s up to 15 s.

Surface Analysis

The Surface Energy Evaluation System—"*See System*" (Advex Instruments, Czech Rep.) was used to evaluate contact angles of 1 µl sessile droplets of distilled water. Usually, around 10 water contact angle values were measured over each sample and four samples were used, for an average value and its deviation. The water contact angles for all glass samples were taken 5 s after the droplets deposition.

XPS spectra were recorded by a hemispherical Phoibos 100 analyser (Specs GmbH, Germany) at a 90° take-off angle and the spectra were referenced to the peak of aliphatic C–C bonds at 284.5 eV. An electron flood gun was not used for charge compensation. An

XR-50 (Specs GmbH, Germany) non-monochromatic X-ray source, with a spectral line Al Kα (photon energy 1,486.6 eV), was used to induce photoelectron emission. High resolution spectra of C1s were recorded, to obtain the chemical bonding statistics of C species. An elemental composition was evaluated from a survey spectra and the relative sensitivity factor (RSF), used for carbon in C1s peak equalled 1.00. CasaXPS software was used for computer processing of the spectra.

The background in Shirley shape was used and C1s peaks were deconvoluted by commonly used Gauss–Lorentz lines, mixed in a 70:30 ratio. For the XPS measurements, the DCSBD apparatus was moved close to the XPS instrument, to minimize essential exposures of samples to atmospheric conditions after the treatment, before inserting the samples into the XPS load-lock chamber. The transportation time was approximately 5 min.

Results and Discussion

Glass–Plasma Influence

The DCSBD plasma consisted of two optically different segments, generated in region 1 and region 2, located above the electrodes on the dielectric surface and between the electrodes on the dielectric surface, respectively. As is indicated by white arrows in Fig. 4, in region 1 and in region 2, diffuse and filamentary plasma were generated, respectively. The white axes, shown in Fig. 4, indicate the positions of selected electrodes which were embedded in dielectric. The influence of glass on the DCSDB plasma spatial properties, in respect to glass–ceramic distance z, is also shown in Fig. 4. The decrease of glass–ceramic distance from $z = 0.75$ mm, which can be considered a point where no interaction of plasma and glass occurred, led to changes in width w of the diffuse plasma in region 1. In Fig. 4, the yellow corridors at locations where $z_1 = 0.68$ mm, $z_2 = 0.38$ mm and $z_3 = 0.09$ mm, shows the width of diffuse plasma $w_1 = 1.18$ mm, $w_2 = 1.48$ mm and $w_3 = 1.73$ mm, respectively.

It is apparent that the decrease of glass–ceramic distance z led to an increase of the diffuse plasma width w. Figure 5 shows that the function between glass–ceramic distance z and diffuse plasma strips width w is linear. It is clear that the glass pane, inserted into DCSBD plasma, is enhancing the diffuse plasma in region 1, at the expense of the filamentary plasma in region 2. When the glass–ceramic distance z is larger than approximately 0.75 mm, the width $w_{\min} = 1.1$ mm corresponds to no glass-plasma interaction. On

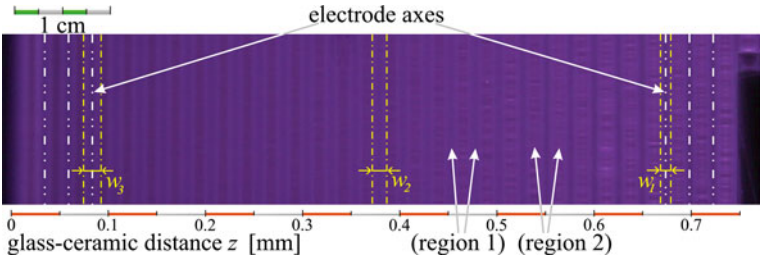

Fig. 4 Photograph of interaction between DCSBD plasma and glass surface, with respect to glass–ceramic distance z (Color figure online)

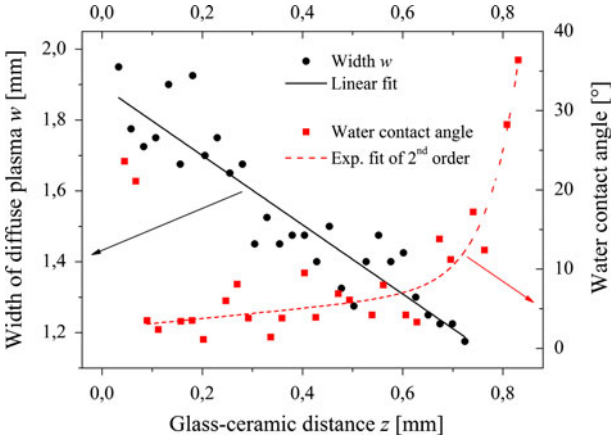

Fig. 5 Width w of DCSBD diffuse plasma and water contact angle on glass surfaces, as a function of glass–ceramic distance z

the other hand, the glass–ceramic distance $z \approx 0.05$ mm corresponds to the highest width of diffuse plasma $w_{max} = 2$ mm.

This phenomenon can be explained by the different mechanism of electric breakdown, which is mainly defined by an inter-electrode distance d and a pressure p. An inter-electrode distance d, or „gas gap", is an important parameter affecting the breakdown voltage and also the ionisation mechanism in plasma. In general, the ionisation mechanism and character of electric breakdown is proportional to $p \times d$ [28]. Since, in the DCSDB electrode arrangement, electrodes are embedded in dielectric, the inter-electrode distance d is fixed. The only parameter that represents the dimension of the space where the electric discharge can occur, is the glass–ceramic distance z.

To explain this peculiarity more clearly, a planar volume-DBD was used to demonstrate the effects of different discharge onsets with respect to the inter-electrode distance d. Figure 6 shows a different behaviour of volume-DBD plasma and it is obvious that $d \approx 0.25$ mm is a boundary for the generation of diffuse ($d < 0.25$ mm) and filamentary ($d > 0.25$ mm) plasma. The reasons behind different behaviours of plasma consist in different breakdown mechanisms related to the inter-electrode distance d. Within a small gap ($d < 0.25$ mm), the single electron avalanche cannot produce a sufficient amount of electrons and fulfil the Meek's breakdown condition for streamer formation [29–31].

However, when the electron avalanche produces enough electrons ($\sim 10^8$) the Meek's criterion is fulfilled and this leads to streamer formation that exhibits as a filamentary plasma. According to [32, 33], the discharge breakdown mechanism differs at $p \times d$ value about 30 Torr.cm. This is in agreement with the observation in Fig. 6, where for $d \approx 0.25$ mm, the $p \times d$ yields about 20 Torr.cm. Therefore, when the glass was placed very close to the DCSBD ceramic (as is shown in Fig. 4), the evolution of streamers (filaments) was quenched by the need of wider space and predominantly, the diffuse plasma in region 1 was observed.

Additionally the glass exhibits as a non-conductive boundary in the plasma and this can lead to the development of an ambipolar electric field, due to a gradient in the concentration of charged particles [34]. The change in electric field distribution may also influence the DCSDB plasma. A similar effect was observed when ITO coated glass panes were introduced into DCSBD plasma [35], instead the regular non-conductive glass pane

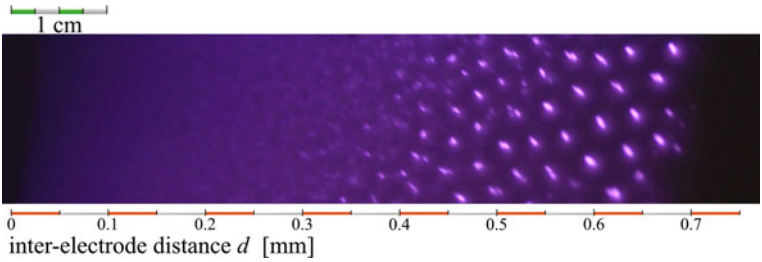

Fig. 6 Photograph of air volume-DBD of various inter-electrode distance d

reported here. However, this leads to the total extinction of filamentary plasma and only diffuse plasma remains present.

Wettability

Surface wettability also relates to adhesion and free surface energy is an important surface property. In general, higher surface energies usually lead to higher adhesion between two different materials. The changes in the surface energy of glass can be observed on the contact angles of water droplets on the glass surface before and after the plasma cleaning process. Contact angles of water droplets are mostly related to the polar (acid–base) [36] part of free surface energy and because, the trend is to use more environmentally friendly water-based coatings [37], the water contact angle provides important information on the efficiency of the plasma cleaning process.

The homogeneity of plasma treatment in static and dynamic treatment modes was investigated regarding spatial changes in wettability. Since the effect of plasma treatment was not clearly visible in photographs, the amorphous SiO_2 coating was applied on the glass surface to increase the water contact angle from 37° to 65°, measured on untreated (2-propanol pre-cleaned) and SiO_2 coated glass, respectively.

After the static plasma treatment for 5 s at $z = 0.3$ mm, the SiO_2 coated glass was immersed in water and then removed to observe the homogeneity of the water film. Figure 7a illustrates that the water layer remained only on diffuse plasma treated segments, whereas the rest of the surface was not sufficiently hydrophilized. This finding is important, because it indicates that diffuse plasma plays a key role in the hydrophilization of glass surfaces, whereas the effect of filamentary plasma is negligible.

Figure 5 also shows the water contact angle as a function of a glass–ceramic distance z. It is obvious that the water contact angle was significantly reduced for $0.1 \text{ mm} < z < 0.6$ mm. The decrease in water contact angles with respect to glass–ceramic distance z can be explained by the increase of the diffuse plasma area (the increase of width w), which resulted in greater efficiency of the DCSBD plasma treatment. With respect to maximal efficiency of treatment and technological convenience in adjusting such small distances, the following experiments were performed at $z = 0.3$ mm.

Since Fig. 4 shows that, at $z < 0.1$ mm, the DCSBD operates in its most effective mode, with the highest values of w, an apparent discrepancy on water contact angles in Fig. 5 was found for $z < 0.1$ mm, where the water contact angle values were unexpectedly high. This can be explained by our observation that at $z \sim 0.1$ mm, there is a 1–2 s delay in plasma onset, exclusively under the area of the treated sample, which resulted in less effective treatment and a higher water contact angle. Even though the DCSBD plasma exhibits most

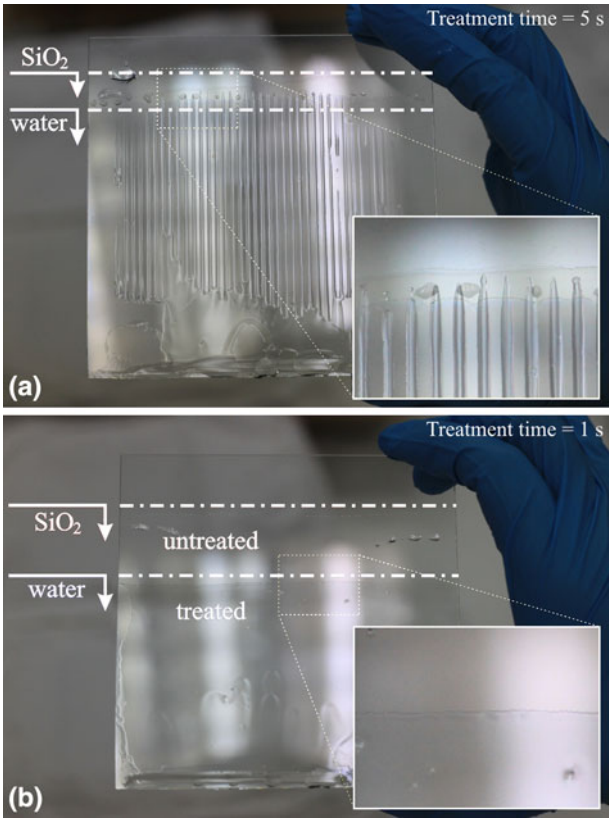

Fig. 7 **a** Non-uniform water film on SiO_2 coated glass, as a result of static DCSBD treatment. **b** Uniform water film on SiO_2 coated glass, as a result of dynamic DCSBD treatment

diffusion for $z \sim 0.1$ mm, this observation shows a limitation of DCSBD plasma for glass cleaning at short treatment times, such as 1–2 s at $z \sim 0.1$ mm.

To eliminate the above issues related to non-homogeneous treatment, in the following experiments we used the dynamic treatment mode. To verify the homogeneity of dynamic treatment, an SiO_2 coated glass was treated in plasma for 1 s at $z = 0.3$ mm, immersed in water and subsequently removed. Figure 7b shows that this led to the formation of a uniform film of water on the plasma treated portion of the SiO_2 coated glass.

Additionally, comparisons in wettability of glass surfaces after 1 s of treatment, in static and dynamic mode, showed a water contact angle about 16° [38] and lower than 3°, respectively. In light of these findings, i.e. wider diffuse plasma strips, followed by a higher efficiency and uniformity of treatment, the DCSBD dynamic treatment provided better results than static treatment.

The phenomenon related to degradation of wettability improvement achieved after plasma treatment, known as the ageing effect, was investigated. Figure 8 shows that the water contact angle on glass cleaned by DCSDB plasma for 6 s, gradually increases with storage time and asymptotic values were reached after about 4 days. The ageing effect or hydrophobic recovery is well described for various surfaces treated by plasma, e.g. polymers [39, 40], paper [41] and metals [42, 43]. Its dynamic is strongly affected by the

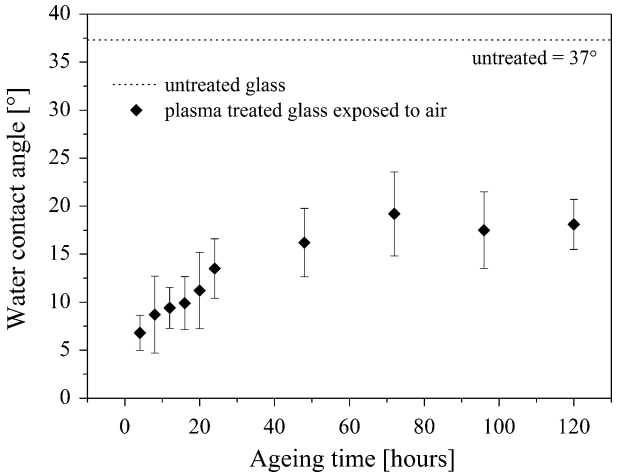

Fig. 8 Stability of the glass surface treated for 6 s, by plasma at power 400 W, stored in ambient air conditions

environment, humidity [44] and temperature [45]. The main reason for surface hydrophobic recovery of surfaces treated by plasma, is carbon contamination from ambient air and transformation of hydrophilic groups in the near surface layer [46, 47].

The surface treatment by plasma generated, using a coplanar arrangement of electrodes, appears to be more effective in increasing glass hydrophilicity than other treatments, where atmospheric pressure air plasma is used to modify glass surfaces, as for example in the treatment by air volume-DBD plasma [21]. The water contact angle shows a decrease from 45° to 10° after plasma treatment for 10 s, to 5° after plasma treatment for 30 s and ultimately to less than 4° after plasma treatment for 60 s. A volume-DBD used in the surface treatment of glass surfaces is also presented in [48]. The water contact angle shows a decrease from approximately 70° to 10° after plasma treatment for 60 s. Since the DBD's in [21, 48] generate a filamentary plasma, it is clear that the greater efficiency of DCSBD is also due to diffuse plasma, which is the major benefit of the DCSBD.

XPS Analysis

The XPS technique was used to investigate changes in surface chemistry before and after the plasma treatment of glass. The C/Si ratio was also used to study the cleaning effect of the DCSBD. The carbon concentration and C/Si ratio on pre-cleaned glass samples, by 2-propanol, were found to be higher than on as-received glass samples, as is shown in Table 1. We also noticed a scatter in carbon concentrations of 2-propanol pre-cleaned samples from 11 to 15 at.% (not shown in Table 1). Regardless of this fact, we assigned a 15 at.% carbon concentration value for 2-propanol pre-cleaned glass.

We found that the DCSBD plasma treatment for 3 s led to a decrease of carbon concentration and C/Si ratio from 15 to 4 at.% and from 0.69 to 0.15, respectively. The C/Si ratio 0.15 and carbon concentration 4 at.% represent the minimal values found after DCSBD plasma treatment and prolonged plasma treatment times had no additional decreasing effect on C/Si ratios and carbon concentrations.

Table 1 Elemental composition of glass surfaces in atomic concentrations as detected by XPS for samples pre-cleaned by 2-propanol and samples cleaned by DCSBD plasma over various times

Sample designation	Concentration (%)								
	C1s	O1s	Si2p	Ca2p	F1s	Mg2s	Na1s	Sn3d 5/2	C/Si
Pre-cleaned in 2-propanol	15	50	21	2	2	3	7	0	0.69
Cleaned in plasma for 1 s	13	55	19	3	2	4	3	2	0.67
Cleaned in plasma for 3 s	4	60	27	2	1	3	2	0	0.15
Cleaned in plasma for 6 s	4	58	27	2	2	5	2	1	0.14
Cleaned in plasma for 9 s	5	60	26	2	2	4	2	0	0.15
Cleaned in plasma for 12 s	4	60	27	2	1	4	2	0	0.16
Cleaned in plasma for 15 s	4	61	26	2	1	4	1	0	0.15

The concentration of silicon was increased after DCSBD plasma treatment for 3 s from 21 at.% to 27 at.%. Since the carbon concentration decreased, an increase in silicon concentration was expected. The concentrations of Na listed in Table 1 showed that Na was decreased from 7 to 3 at.% and 1 at.%, after plasma treatment of samples treated for 3 and 15 s, respectively. The plasma treatment had no significant effect on concentration of the rest of the elements of which glass surfaces consist, as Ca, F, Mg, Sn that are also shown in Table 1.

The oxygen concentration was increased after plasma treatment for 3 s from approximately 50 to 60 at.%. Higher concentrations of oxygen can be related to another phenomenon, since the plasma treatment can possibly generate oxygen-based functional groups [21] on surfaces, as a detailed analysis of C1s high-resolution peak showed.

The C1s peak was deconvoluted into three main components, as is shown in Fig. 9, where full width at half maximum (FWHM) are also written. The peaks at binding energies 284.5, 286.0 and 288.0 eV were attributed to C–C or C–H, C–O and O–C=O with reasonable FWHM, respectively [49, 50]. Plasma treatment for 3 s decreased C–C or C–H bond concentrations, while the bond concentrations of C–O and O–C=O increased, as is shown on C1s peak in Fig. 9.

The C–C and C–H bonds concentrations were decreased from an initial 74 to 48 % after plasma treatment for 3 s. Since the C–C and C–H bonds are related with the initial surface hydrocarbon contaminants, this shows that plasma treatment exhibits a cleaning effect on glass surfaces. The concentrations of C–O and O–C=O were increased from 13 to 28 % and from 13 to 24 %, respectively, after plasma treatment for 3 s. This result indicates that the plasma governed the glass surface by polar oxygen-based groups such as C–O, C=O, O–C=O or COOH. Since water has a polar character, this can also contribute to explaining the decrease of water contact angle values after plasma treatment.

Figure 10 shows that prolonging plasma treatment times from 3 up to 15 s had a different influence on carbon bonds concentrations than shorter treatments up to 3 s. Figure 10 illustrates that the biggest change in carbon bonds concentration was achieved after plasma treatment for 3 s. Following plasma treatments up to 15 s changed the C–C and C–H concentration back towards the original concentrations and remained at approx. 60 %. Also a different behaviour of O–C=O concentration was found after 3 s of plasma treatment and decreased back to its original concentration of approx. 13 %. However, a significantly slower increase was found in C–O bonds concentration development after 3 s of plasma treatment, with only C–O showing the same trend during the entire plasma

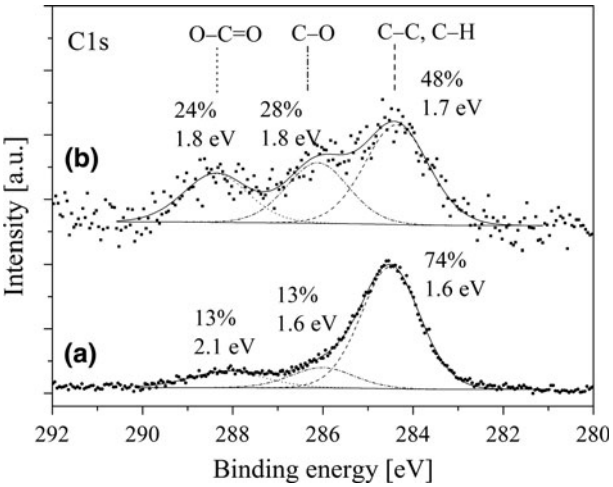

Fig. 9 Deconvolution of C1 s peak for (**a**) untreated glass samples and (**b**) 3 s plasma treated glass samples, the individual bond abundances and FWHMs indicated

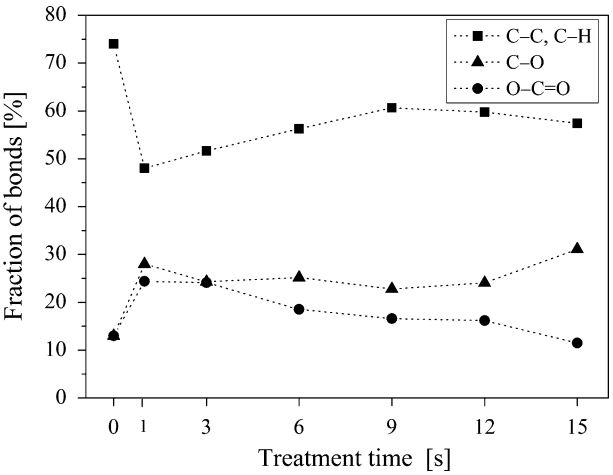

Fig. 10 Evolution of C1 s states on glass surfaces in respect to plasma treatment times

treatment process. C–O concentration was found to be approx. 30 % after plasma treatment for 15 s.

There is an indication that the efficiency of the DCSBD plasma for glass cleaning can be even higher than is presented here, because the experiments were not done in situ. It is possible that the measured surface carbon concentration of approx. 4 at.% was adsorbed from the environment during transportation from the DCSDB apparatus to an XPS load-lock chamber. Although the samples were transported into the XPS load-lock chamber as quickly as possible, at least a few minutes was necessary.

Ref. [51] shows an XPS study of the surface chemistry of glass in a vacuum. It was found that an exposure of the ultra-clean glass surface to an ambient air atmosphere for

2 min, increases the carbon concentration from approx. 0.5 to 3–5 at.%. These results also show that accumulation of carbon contaminants concentrations are a strongly non-linear function of air exposure times and the highest rate is in first 2 min of exposure. The C/Si ratio after 2 min of ambient air exposure is 0.2, which is in good agreement with the observed C/Si ratio 0.15 reported here, where plasma treated glass was exposed to ambient air during transportation from DCSBD apparatus to an XPS load-lock chamber. Therefore the similar C/Si ratios measured for various glass samples treated in plasma, in respect to treatment times, (see Table 1) can be explained by high carbon contamination rates from ambient air.

Conclusion

In this study, we illustrated the effective treatment of flat glass surfaces using diffuse ambient air plasma generated by DBD of coplanar electrode arrangement—the DCSBD. The DCSBD plasma treatment for 1 s had a significant effect on the wettability of glass surfaces. Water contact angles decreased from an initial 37° to less than 3°. XPS measurements showed that, after plasma treatment, the carbon concentration on glass was reduced from 15 to 4 at.%. Prolonged plasma treatment times, up to 15 s, had no further effect on carbon concentration. The deconvolution of C1s peak showed higher concentrations of polar oxygen-based functional groups after the plasma treatment which, together with cleaning, play an important role in the wettability of glass surfaces.

Acknowledgments This work was supported by the project R&D Centre for Low-Cost Plasma and Nanotechnology Surface Modifications—CZ.1.05/2.1.00/03.0086 funding by the European Development Fund, the Slovak Research and Development Agency, Project. No. APVV-0491-07, and by the Czech Science Foundation (GACR) project GAP205/10/0979.

References

1. Axinte E (2011) Mater Des 32:1717–1732
2. Inoue T (2003) Energy Build 35:463–471
3. Mohelnikova J (2009) Constr Build Mater 23:1993–1998
4. Cras J, Rowe-Taitt C, Nivens D, Ligler F (1999) Biosens Bioelectron 14:683–688
5. Lim SW (2003) Jpn J Appl Phys 42:5002–5009
6. Angermann H, Henrion W, Rebien M (2004) Appl Surf Sci 235:322–339
7. Han Y, Mayer D, Offenhausser A, Ingebrandt S (2006) Thin Solid Films 510:175–180
8. Bell KL, Dalgarno A, Kingston AE (1968) J Phys B At Mol Opt 1:18–22
9. Xu X (2001) Thin Solid Films 390:237–242
10. Kogelschatz U, Eliasson B, Egli W (1999) Pure Appl Chem 71:1819–1828
11. Gibalov V, Pietsch G (2000) J Phys D Appl Phys 33:2618–2636
12. Iwasaki M, Matsudaira Y, Takeda K, Ito M, Miyamoto E, Yara T, Uehara T, Hori M (2008) J Appl Phys 103:023303-1–023303-7
13. Šimor M, Ráheľ J, Vojtek P, Černák M, Brablec A (2002) Appl Phys Lett 81:2716–2718
14. Zhu AM, Nie LH, Wu QH, Zhang XL, Yang XF, Xu Y, Shi C (2007) Chem Vap Depos 13:141–144
15. Masuda S, Akutsu K, Kuroda M, Awatsu Y, Shibuya Y (1988) IEEE T Ind Appl 24:223–231
16. Langmuir I (1918) J Am Chem Soc 40:1361–1403
17. Paynter R (1999) Surf Interface Anal 27:103–113
18. Buček A, Homola T, Aranyosiová M, Velič D, Plecenik T, Havel J, Sťahel P, Zahoranová A (2008) Chem Listy 102:1459–1462
19. Takahashi H, Sato K, Sakata S, Okada T (1995) J Electrostat 35:309–322
20. Ames D (2004) Surf Coat Tech 187:199–207
21. Yamamoto T, Okubo M, Imai N, Mori Y (2004) Plasma Chem Plasma P 24:1–12

22. Kondoh E, Asano T, Nakashima A, Komatu M (2000) J Vac Sci Technol, B 18:1276–1280
23. Larson B, Helgren J, Manolache S, Lau A, Lagally M, Denes F (2005) Biosens Bioelectron 21:796–801
24. Černák M (2007) Faculty of mathematics, physics and informatics. Comenius University, Slovakia: Patent WO 2007/142612 A1, Slovakia
25. Černák M, Černáková Ľ, Hudec I, Kováčik D, Zahoranová A (2009) Eur Phys J Appl Phys 47:22806-1–22806-6
26. Hoder T, Šíra M, Kozlov KV, Wagner HE (2008) J Phys D Appl Phys 41:035212-1–035212-9
27. Homola T, Matoušek M, Hergelová B, Kormunda M, Wu YLL, Černák M (2012) Polym Degrad Stab 97:886–892
28. Paschen F (1889) Ann Phys 273:69–96
29. Loeb LB, Meek JM (1940) J Appl Phys 11:438–447
30. Loeb LB, Meek JM (1940) J Appl Phys 11:459–474
31. Raizer YP (1991) Gas discharge physics. Springer, Berlin
32. Massines F, Gherardi N, Naudé N, Ségur P (2009) Eur Phys J Appl Phys 47:22805-1–22805-10
33. Brauer I, Punset C, Purwins HG, Boeuf JP (1999) J Appl Phys 85:7569–7572
34. Chen F, Von Goeler S (2006) Introduction to plasma physics and controlled fusion, vol 1: Plasma physics. Springer
35. Homola T, Matoušek J, Medvecká V, Zahoranová A, Kormunda M, Kováčik D, Černák M (2012) Appl Surf Sci 258:7135–7139
36. van Oss C, Chaudhury MK, Good RJ (1988) Chem Rev 88:927–941
37. Pianoforte K (2011) The industrial coatings market: industrial coatings manufacturers express optimism for the coming year. Coatings world. http://www.coatingsworld.com/issues/2011-06/view_features/the-industrial-coatings-market/. Accessed 2011
38. Homola T, Buček A, Zahoranová A, Černák M (2007) 16th annual conference of Doctoral students WDS '07—part II: physics of plasma and ionized media. Prague Matfyzpress 124–128
39. Morent R, De Geyter N, Leys C, Gengembre L, Payen E (2007) Surf Coat Tech 201:7847–7854
40. Kormunda M, Homola T, Matoušek J, Kováčik D, Černák M, Pavlík J (2012) Polym Degrad Stab 97:547–553
41. Pykonen M, Sundqvist H, Kaukoniemi O, Tuominen M, Lahti J, Fardim P, Toivakka M (2008) Surf Coat Tech 202:3777–3786
42. Lin JW, Chang HC (2011) Nucl Instrum Meth B 269:1801–1808
43. Prysiazhnyi V, Cernak M (2012) Thin Solid Films 520:6561–6565
44. Dupont-Gillain CC, Adriaensen Y, Derclaye S, Rouxhet PG (2000) Langmuir 16:8194–8200
45. De Geyter N, Morent R, Leys C (2008) Nucl Instrum Meth B 266:3086–3090
46. Prysiazhnyi V, Zaporojchenko V, Kersten H, Černák M (2012) Appl Surf Sci 258:5467–5471
47. Homola T, Matoušek J, Hergelová B, Kormunda M, Wu LY, Černák M (2012) Polym Degrad Stab 97:2249–2254
48. Wang C, He X (2006) Appl Surf Sci 252:8348–8351
49. Crist BV (2004) Handbook of monochromatic XPS spectra. XPS International LLC, USA
50. Takeda S, Yamamoto K, Hayasaka Y, Matsumoto K (1999) J Non Cryst Solids 249:41–46
51. So L, Ng N, Bilek M, Pigram PJ, Brack N (2006) Surf Interface Anal 38:648–651